IDENTIFICATION OF LOCAL TO GLOBAL MECHANICAL PROPERTIES OF CLEAR WOOD PEELED VENEERS FROM OFF-AXIS TENSILE TESTS USING FULL-FIELD LOCAL DISPLACEMENT MEASUREMENTS

L. Demoulin[1], G. Pot[2], L. Denaud[3], S. Girardon[4] and B. Marcon[5]

[1]Arts et metier Institute of technology, LABOMAP, Université Bourgogne Franche-Comté, F-71250 Cluny, France
Email: leyne.demoulin@ensam.eu, Web Page: https://labomap.ensam.eu/
[2]Arts et metier Institute of technology, LABOMAP, Université Bourgogne Franche-Comté, F-71250 Cluny, France
Email: guillaume.pot@ensam.eu, Web Page: https://labomap.ensam.eu/
[3]Arts et metier Institute of technology, LABOMAP, Université Bourgogne Franche-Comté, F-71250 Cluny, France
Email: louis.denaud@ensam.eu, Web Page: Web Page: https://labomap.ensam.eu/
[4]Arts et metier Institute of technology, LABOMAP, Université Bourgogne Franche-Comté, F-71250 Cluny, France
Email: stephane.girardon@ensam.eu, Web Page: Web Page: https://labomap.ensam.eu/
[5]Arts et metier Institute of technology, LABOMAP, Université Bourgogne Franche-Comté, F-71250 Cluny, France
Email: bertrand.marcon@ensam.eu, Web Page: Web Page: https://labomap.ensam.eu/

Keywords: Digital Image Correlation, Fibre orientation, Density, Young Modulus, Strength

Abstract
This study examines the influence of fiber orientation variability on the mechanical properties of wood, focusing on veneer clear wood specimens. The research is motivated by the need to develop high-performance composite materials for sustainable transportation applications, particularly in reducing greenhouse gas emissions. The experimental protocol involves manufacturing veneers from beech wood, followed by producing the manufacturing of veneers from beech wood, followed by the production of small specimens with deliberate variations in fiber orientation. Non-destructive measurements of local fiber orientations and global density are conducted, along with tensile tests to determine local mechanical properties, i.e., Young's modulus, strength, and the shear modulus Advanced imaging techniques (DIC) and models for isotropic materials are employed for analysis.
The results reveal that fiber orientation has a significant role in wood variability, with pronounced effects on Young's modulus and strength at low angles. Transversal and shear modulus appear lower than in the literature due to the cracks due to the manufacturing of veneer (peeling process).

1. Introduction

The transport industry is determined to reduce its carbon footprint in order to reduce the problems caused by greenhouse gases. To achieve this goal, high-performance materials made from wood could be used for structural applications. This is the rationale behind the WOOFHI (Wood/natural Fiber High homogeneity/performance composite) project, which aims to produce homogeneous, optimized composite materials made from heterogeneous, variable materials. This application requires the ability to sort wood material according to its mechanical properties, based on non-destructive and quantitative

measurement methods. Visual sorting is standardized but not very efficient, and mechanical properties after sorting are not optimal (Faydi 2017, Duriot 2021). Several studies attempt to predict the elastic modulus and mechanical strength of structural wood products accurately and reliably, as shown by Hakkarainen et al. (2019) using local fiber orientation and global density measured on wood (Viguier et al. 2018). The coefficient of determination obtained is less than 0.7 and few predictive studies concerning veneers and small flawless samples have been made (Pramreiter et al. 2021, Cha 2003).

The aim of this work is to understand the mechanical behavior of clear wood and how local disturbances influence the material's behavior.
An experimental protocol on small specimens made from visually "clear" veneers was set up. First, non-destructive measurements of fiber orientation and density were carried out, then the specimens were loaded to failure in a tensile test.

2. Material and methods

2.1. Experimental protocol

The first stage of the protocol concerns the manufacture of veneers from the peeling process. The species studied is beech (fagus sylvatica) from the Centre Val de Loire region. Secondly, test specimens measuring 350 mm long, 20 mm wide, and 2 mm thick were produced from these veneers using a laser cutting machine. The specimens were stored at a temperature of 24°C with a relative air humidity of 50% in order to stabilize them at a humidity of 10%. The specimens were cut at angles relative to a direction assumed to be 0° to deliberately create variability within the fiber orientation. This distribution is shown in Table. 1. Nearly 40 veneers were required to produce 129 specimens.

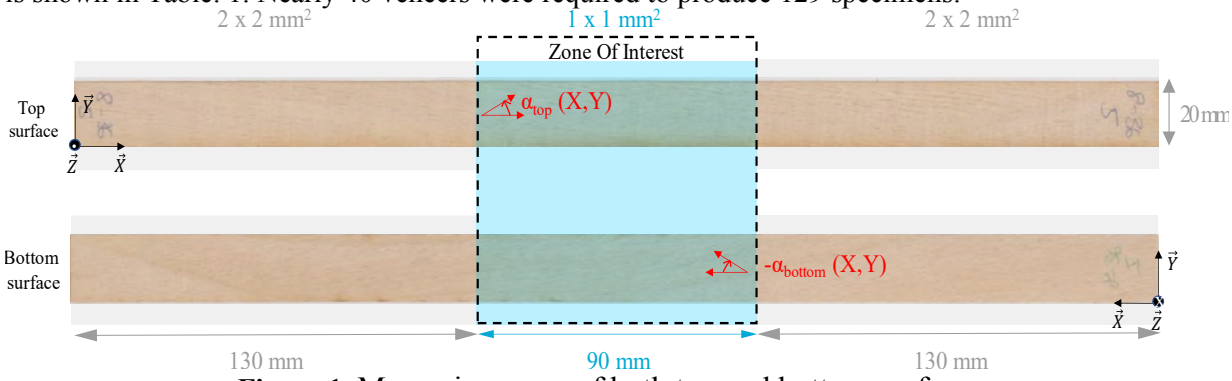

Figure 1. Measuring areas of both top and bottom surfaces

Table 1. Distribution of specimens according to their cutting angle, number of tested specimens, and cross-head speed during the tensile mechanical test

Cutting Angle θ (°)	**0**	**5**	**10**	**15**	**20**	**30**	**45**
Number	40	16	15	11	24	14	9
Cross-head speed (mm.min^{-1})	2	2	1	1	1	0.5	0.5

The samples were then scanned using a machine equipped with a camera and laser pointer, which scanned their entire surface. This technology uses the tracheid effect (Nyström (2003), Simonaho et al. (2002)). This involves projecting a circular laser onto a flat wooden surface. As light scattering is higher in the direction of the wood fiber, a luminous ellipse is formed whose major axis follows this orientation. The top and bottom surfaces of the sample were scanned at different resolutions (Figure. 1) to obtain angle maps (Figure. 2 (a), (c)). The central zone was more highly resolved than the extremities, as this is the zone of interest visible between the tensile jaws. The next step was to scan the specimens using a

conventional scanner to obtain an image with a resolution of 400 Dpi. Figure. 2 shows the overlay of the angle mapping obtained with the scan (Figure. 2(b), (d)).

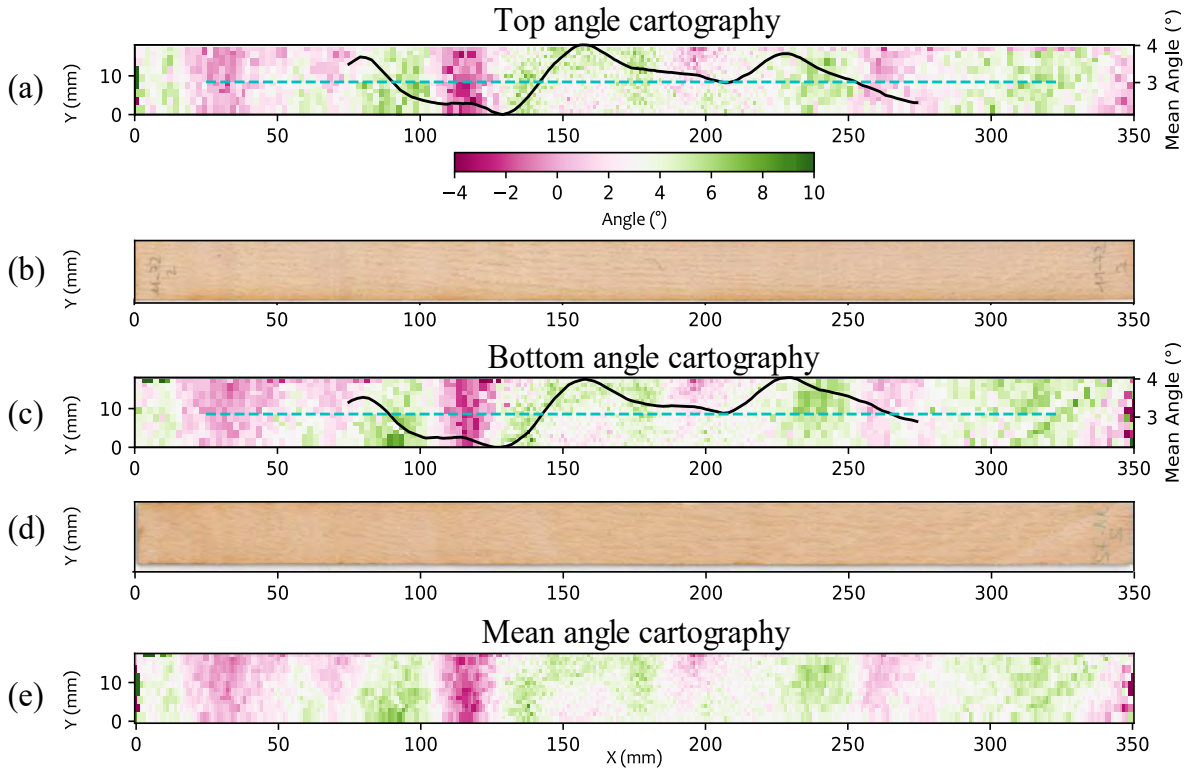

Figure 2. (a) The angle cartography in degrees of the top surface of the specimen. The black curve represents the average value of the grain angle along the Y direction for each X step in the ZOI (Zone Of Interest) with a length of 50 mm, the dashed blue line represents the average angle value within the ZOI (b) color image of the top surface, (c) The angle cartography in degrees of the bottom surface of the specimen, (d) color image of the bottom surface, (e) The average angle cartography in degrees of the top and bottom face angles of the specimen.

Width was measured with a caliper, and thickness with an external micrometer. The samples were then weighed using a balance. These measurements were used to calculate the average density. The tensile test was designed to determine local mechanical properties using a ZWICK-Roell, universal testing machine (250 kN). Displacements were measured by image stereo-correlation using technology developed by LaVision. A preload of 0.1 MPa was applied before testing. The displacement speeds imposed on the specimens are described in Tab.1. Speeds were set to give a test time of between 100 and 180 s to failure.

2.2. Young modulus determination

The equivalent local modulus of elasticity along the specimen can be calculated using a virtual extensometer of length δ (Figure. 3). This modulus was calculated based on the standard (EN 408 2012), i.e. a linear regression is calculated between 10 and 40% of the estimated maximum force.

In the $\vec{X}$ direction, the elastic modulus is calculated according to Eq. 1. Strain was calculated as a rate of increase in displacement as shown in Eq. 2. Displacement was calculated as the average of displacements over the width of the specimen (yellow bands (Figure. 3). Stress is the ratio of force divided by specimen cross-section (Eq. 3). Using this method, a local modulus can be calculated at each point along the length of the specimen. The central zone can be scanned over the 90 mm length of the zone of interest using the virtual extensometer with a length δ = 50 mm. The type of results obtained for one specimen is shown in Figure. 4.

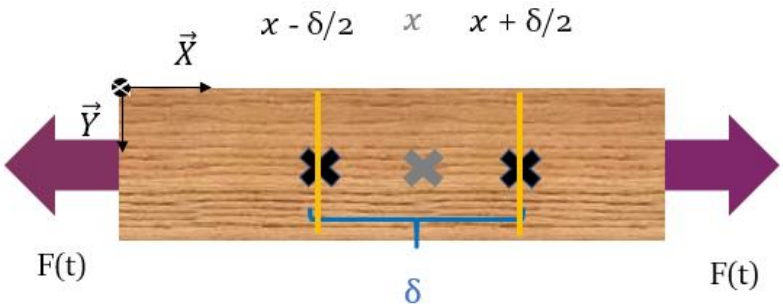

Figure 3. Tensile test with x the position along the length of the specimen at the center of the extensometer, δ the length of the extensometer and F(t) the force as a function of time.

$$E_{xx}(x) = \frac{\sigma}{\varepsilon_{xx}(x)} \quad (1)$$

$$\varepsilon_{xx}(x) = \frac{u(x+\delta/2) - u(x-\delta/2)}{\delta} \quad (2)$$

$$\sigma = \frac{Force}{Section} \quad (3)$$

$$u(x) = \frac{1}{19-1+1}\sum_{i=1}^{19} u(x, y_i) \quad (4)$$

Where $E_{xx}(x)$, $\varepsilon_{xx}(x)$ and σ are respectively the young modulus (in GPa), the strain in the $\vec{X}$ direction, and the stress (in MPa). The force is in N and the section in mm. $u(x)$ is the mean displacement in mm on the yellow band (Figure 3).

2.3 Strengh

Models of mechanical strength using grain angles can be used, such as the Hankinson (1921), Norris (1962), and Tsai-hill (1965) models as shown respectively by Eq. 5, Eq. 6, and Eq. 7.

$$\mathrm{MOR}_H = \frac{F_L \times F_T}{F_L \times \sin(\alpha)^2 + F_T \times cos(\alpha)^2} \quad (5)$$

$$\mathrm{MOR}_N = \frac{1}{\sqrt{\frac{1}{{F_T}^2} \times \sin(\alpha)^4 + \frac{1}{{F_L}^2} \times \cos(\alpha)^4 + (\frac{1}{{f_v}^2} - \frac{1}{F_L * F_T}) \times \sin(\alpha)^2 \cos(\alpha)^2}} \quad (6)$$

$$\mathrm{MOR}_{TH} = \frac{1}{\sqrt{\frac{1}{{F_T}^2} \times \sin(\alpha)^4 + \frac{1}{{F_L}^2} \times \cos(\alpha)^4 + (\frac{1}{{f_v}^2} - \frac{1}{{F_L}^2}) \times \sin(\alpha)^2 \cos(\alpha)^2}} \quad (7)$$

Where F_L and F_T are respectively the tensile strength in the longitudinal, transversal direction (in MPa) and f_v the ultimate shear strength in the plane LT (in MPa) and α is the angle (in degree).

3. Results

3.1 Young modulus

The results obtained for each specimen are shown in Figure. 4, which illustrates the strong correlation between the longitudinal modulus of elasticity and the angle at each point on the map. By superimposing all the specimens on the same graph, the mechanical properties have been determined by considering an orthotropic behavior law (Figure. 5). The longitudinal modulus of 16.14 GPa appears to agree with the literature (OŻYHAR et al. 2012, Ozyhar et al. 2013, Peter et al. 2015) despite a relatively low transverse

modulus and shear modulus, possibly indicating the considerable influence of cracks resulting from the veneer manufacturing process (Pot et al. 2015, Krüger et al. 2023). Moreover, a wide range of the MOE is observed (from 12 to 20 GPa). This variability may stem from density, microfibril angle, tension wood, or the presence of out-of-plane angles.

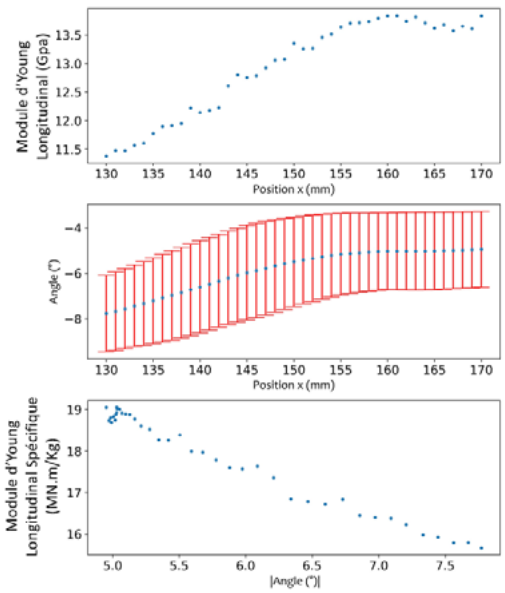

Figure 4 : Example of a specimen result: longitudinal modulus and angle measurement as a function of position along the length of the specimen, specific longitudinal modulus as a function of angle

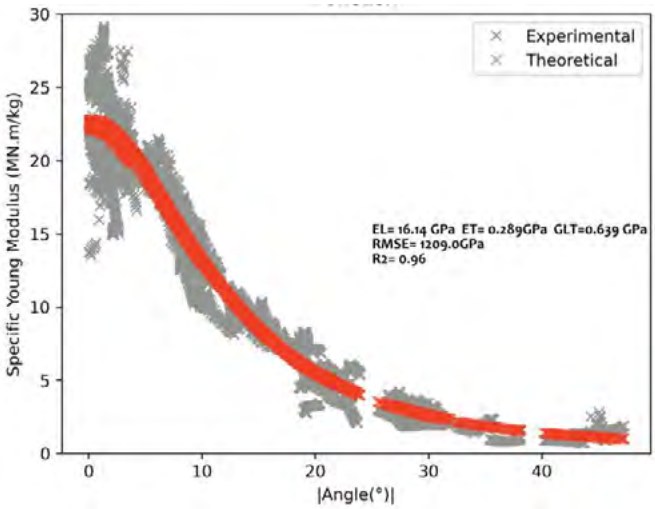

Figure 5 : Optimization and superposition of mechanical properties based on an orthotropic behavior law (RMSE = Root Mean Square Error, R2 = coefficient of determination, EL = longitudinal modulus and ET = transverse modulus, GLT = shear modulus)

3.2 Strength

The relationship between the mean absolute angle and the strength (MOR) within the length of the ZOI measured in step 4 is depicted in Figure 6. Hankinson, Norris, and Tsai-Hill failure criteria (respectively Eq. 5, 6, and 7) were fitted to the experimental data, giving the coefficients in Table 2.

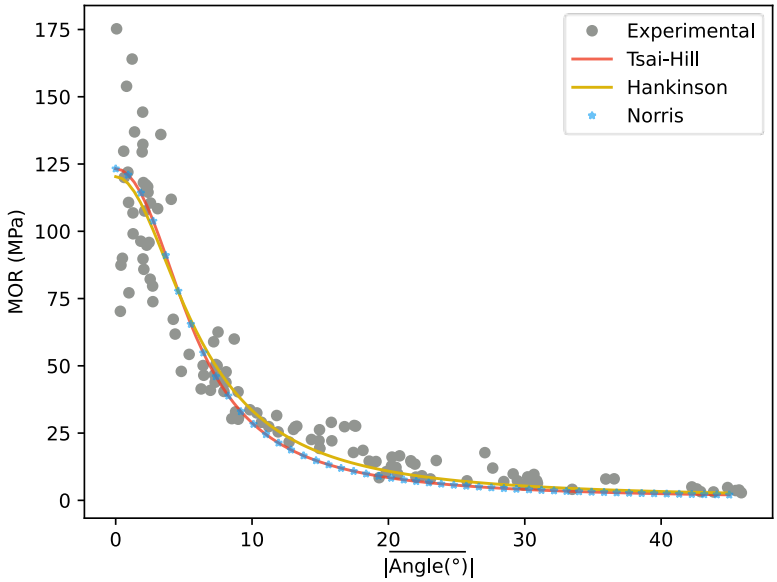

Figure 6: MOR VS $|\overline{Angle}|$

MOR correlates quite well with the measured angle in the ZOI with the three models (Figure 6 and Table 2). For angles close to 0°, there was a wide variation in MOR. The Hankinson (1921) model has a coefficient of determination which is the highest. However, this model only provides longitudinal and transverse mechanical strength, in contrast to the Tsai-Hill (1965) and Norris (1962) models, which also allow to evaluate a shear strenght.

Table 2. Coefficients of rupture models.

Model/Coefficient	F_L (MPa)	F_T (MPa)	f_v (MPa)	R^2	RMSE (MPa)
Hankinson	121	1.0	-	0.90	14.1
Norris	123	1.0	8.0	0.88	15.0
Tsai-Hill	125	1.0	14.0	0.89	15.0

4. Conclusion

Fiber orientation appeared to be an important parameter in wood variability for the young modulus and tensile strength. Large variations in young modulus and strength were more significant for small angles than for large angles. These variations could be due to the locale variation of the density, the out-of-plane angle, or the microfibril angle.
The approach of calculating elastic modulus is rather simplistic for understanding local behavior. Inverse identification of mechanical properties for each specimen using a finite element model incorporating fiber orientation seems essential to understanding strains and local properties.

Acknowledgments

This work is supported by the "Investissement d'Avenir" program, ISITE-BFC project (ANR-15-IDEX-003 contract).

References

[1] Azzi VD, Tsai SW (1965) Anisotropic strength of composites: Investigation aimed at developing a theory applicable to laminated as well as unidirectional composites, employing simple material properties derived from unidirectional specimens alone. *Experimental Mechanics* 5:283–288. https://doi.org/10.1007/BF02326292
[2] Cha J-K (2003) Tensile Strength of Clear Thin Wood Samples in Relation to the Slope of Grain. Journal of the Korean *Wood Science and Technology*. 2003. Vol. 31, n° 3, pp. 35-41.
[3] Duriot R (2021). *Développement de produits LVL de douglas aux propriétés mécaniques optimisées par l'exploitation de la mesure en ligne de l'orientation des fibres lors du déroulage* Thèse de doctorat. HESAM.
[4] EN 408 (2012). *Timber structures – Structural timber and glued laminated timber – Determination of some physical and mechanical properties*.
[5] Faydi Y (2017) *Classement pour la résistance mécanique du chêne par méthodes vibratoires et par mesure des orientations des fibres*. Thèse de doctorat. ENSAM.
[6] Hankinson (1921) Investigation of crushing strength of spruce at varying angles of grain. *Air service information circular* 3:16
[7] Krüger R, Buchelt B, Wagenführ A (2023) Method for determination of beech veneer behavior under compressive load using the short-span compression test. *Wood Science and Technology* 57:1125–1138. https://doi.org/10.1007/s00226-023-01489-z
[8] Nyström J (2003) Automatic measurement of fiber orientation in softwoods by using the tracheid effect. *Computers and Electronics in Agriculture* Vol. 41, n° 1-3, pp. 91-99. DOI 10.1016/S0168-1699(03)00045-0.
[9] Ozyhar T, Hering S, Niemz P (2012) Moisture-dependent elastic and strength anisotropy of European beech wood in tension. *Materials Science* 47:6141–6150. https://doi.org/10.1007/s10853-012-6534-8

[10] Peter N, Tomasz O, Stefan H, Walter S (2015) Moisture dependent physical-mechanical properties from beech wood in the main directions. *Pro ligno* https://doi.org/10.24451/ARBOR.5636

[11] Ozyhar T, Hering S, Niemz P (2013) Moisture-dependent orthotropic tension-compression asymmetry of wood. *Holzforschung* 67:395–404. https://doi.org/10.1515/hf-2012-0089

[12] Pot G, Denaud LE, Collet R (2015) Numerical study of the influence of veneer lathe checks on the elastic mechanical properties of laminated veneer lumber (LVL) made of beech. *Holzforschung* 69:247–316. https://doi.org/10.1515/hf-2014-0011

[13] Pramreiter M, Stadlmann A, Huber C, Konnerth J, Halbauber P, Baumann G, Mülher U (2021) The Influence of Thickness on the Tensile Strength of Finnish Birch Veneers under Varying Load Angles. *Forests*.Vol. 12, n° 1, pp. 87. DOI 10.3390/f12010087.

[14] Simonaho S-P, Silvennoinen R (2002) Determination of wood grain direction from laser light scattering pattern. *Optics and Lasers in Engineering*. 2002. Vol. 41, n° 1, pp. 95-103. DOI 10.1016/S0143-8166(02)00144-6.

[15] Viguier J, Bourgeay C, Rohumaa A, Pot G, Denaud L (2018) An innovative method based on grain angle measurement to sort veneer and predict mechanical properties of beech laminated veneer lumber. *Construction and Building Materials*. Vol. 181, pp. 146-155. DOI 10.1016/j.conbuildmat.2018.06.050. ACL